Namibian Journal for Research, Science and Technology

Vol 2, December 2020

Estimating the Rainfall Patterns in Namibia: Are rainfall patterns a myth or fact?

[1]H.J. Sartorius von Bach & [2]K.M Kalundu

[1]Department of Agricultural Economics, Faculty of Agriculture and Natural Resources, University of Namibia
[2]Department of Agricultural Economics, Faculty of Agriculture and Natural Resources, University of Namibia

svonbach@unam.na; Tel: +264 (61) 206 4043
skalundu@unam.na; Tel: +264 (61) 206 4015

ARTICLE INFO

Article History:

Received: March 2020
Published: December 2020

Keywords:

Cycles, El Niño, forecast, oscillation index, Namibia, rainfall pattern

ABSTRACT

Rainfall is generally regarded as the key driver for ecosystem processes, particularly important within the dynamics of semi-arid regions. Since the precipitation impacts the natural environment, human society and the economy, the paper applied rainfall forecasting to avail early warning patterns. The Waterberg rainfall data from 1895 to 2019 was used to determine a better understanding of its pattern. This is necessitated because knowledge of rainfall patterns are required for reviewing production targets and a necessity for decision making in agriculture. Data shows that only 34% of the rainfall years accounted average rainfall, meanwhile 66% of rainfall years is either classified as above or below. Further, results show that the ENSO patterns follow a cyclical pattern, which corresponds to the local Waterberg rainfall. Econometric approaches postulate that there exists volatility of rainfall, effective rainfall, its intensity, cycles and the ENSO data. This paper shows that rainfall forecasting is possible when using a model that takes into account the variation in the ENSO, cyclical pattern and the accumulation of various rainfall cycles. A five year forecast shows that the current experienced drought cycle is coming to an end, and that the prospects of above average years will only persist for 2 years. We recommend that knowledge of the cyclical trend needs to be translated into reliable periodic statements to safeguard Namibia against future famines, possible food shortages and counter rising food prices. Although the methods are robust, they call for further research into the causes of dynamics of observed rainfall variability.

Introduction

Rainfall is generally regarded as key driver of ecosystem processes (Anderson et. al., 2007), and especially important within the vegetation dynamics of semi-arid regions. Because of the historic precarious circumstances, climate forecasting has been an active area of research since Sir Gilbert Walker discovered a relationship between large-scale atmospheric variability and rainfall in many parts of the world (Walker, 1923). Research emerged into weather forecast models, and scientists begin to understand weather and specifically rainfall patterns. The demand for seasonal rainfall forecasts has been increasing, and their usage has been established, for instance in water resources, food security, and coastal zone management (Cottrill et. al. 2013). Nowadays, the El Niño–Southern Oscillation (ENSO) is generally followed to detect the beginning of a cycle and its severity through models, such as seasonal performance probability (SPP) for Africa (Novella & Thiaw, 2016). It avails weather information, thus providing crucial information for decision-making across different sectors (for example, Pal et. al. 2013; Siegmund et. al. 2015). Already in 2012, meteorologists forecasted that southern Africa was entering a severe drought period consisting of 10 years. Unfortunately, this early warning was not followed and together with global warming, triggered activities with substantial negative direct impacts on the Namibian agriculture and indirectly on the regional economy at large.

The purpose of this contribution therefor is to identify rainfall patterns and call for the incorporation ENSO effects into the planning and execution of national agenda.

An early prediction and warning depend on the predicted rainfall amount (Winsemius, 2014, and Becker et. al., 2014), which has always been challenging to accurately forecast rainfall in practical (Hirata & Grimm, 2018). It is believed that once the pattern is known, Namibian agriculture could benefit. Since the precipitation impacts on the natural environment, human society and the economy is affected. The question to be asked is how the rainfall affects the economic activities, since a drought can be defined differently from metrological, agricultural or hydrological perspectives. To assess the rainfall patterns, this paper will use metrological rainfall time series to investigate the existence of cyclical patterns, important for an early warning system. This could support sectors to know the beginning of an agricultural drought (Mishra & Singh, 2010). The vegetation requirements depend on availability of water, and not necessarily on rainfall. Therefore, the drought does not necessarily begin on the day that rain ceases, but rather when the soil moisture is drained. This brings us to the deficiency in total water supply as compared to the total water demand, which require knowledge of the general weather pattern, being more important than individual occurrences. It implies, that if the reservoir is filled, one dry period will not result into a drought, since the drought is only the consequence of the accumulated years' effect. This principle not only occurs to water, but also to food security, environmental degradation, and economic hardship, knowledge on seasonal precipitation is important to provide an early warning to determine the occurrence of drought or non-drought situations (Lin et. al., 2016).

Historic review on rainfall patterns

Rainfall patterns existed all time, but analysis generally could use data since the existence of record keeping. Therefore, records of significance for both meteorological factors and streamflow go back at best for 75 to 100 years and in most cases only between 30 to 50 years. Since earlier cycles and patterns are unknown, predictions are limited. This gap was addressed through international research, deriving information on climatic changes from tree rings, ice cores and lake sediments. Various cycles have been identified by Chin (1978). Medium term ice core series for example showed that some 300 years ago a little ice age period persisted for several decades and that for the past 100 years, a relatively warm climate pattern was observed. Longer time span series (Emiliani, 1966) showed that about 5 000 and 6 000 years ago, the world experienced its warmest period recorded. Cycles showed that it took about 40 000 to 70 000 years to reach a glacial maximum; the last one was 18 000 years ago. Chin (1978) showed that it only took between 2 000 to 5 000 years to completely destroy the formed continental-sized ice sheet. Therefore, analysis show that it is likely that we are still in a warm trough within a long-term cycle, i.e. the current climatological variability might continue for at least the next few thousand years.

Focusing on extreme droughts globally, the earliest recorded drought dates back to the year 1540, when probably the worst drought took place in Central Europe without any precipitation for 11 months leading to temperature increases of 5 to 7 degrees above the normal.

Recorded severe droughts occurred in India in 1900, in Russia in 1921, China 1929, southern USA in the 1930's and more recently reported for Kenya, Brazil, Australia, and other countries. On the other hand, excess precipitation showed increased frequency and intensity of extremes (Cohen et. al., 2014). The severity of these events varied. Nevertheless, the overall impact of these events would have been less critical once known to allow protective steps to have been taken place. Research findings from the Karoo, with a similar climate showed that their rainfall, concentration, and its seasonality are not random processes. Findings shows cyclic patterns, with rainfall explained as single or double cycles (Du Toit & O'Connor, 2014). These cyclical patterns are used in decision-making, as in the case of Australia, where pastoralists use seasonal climate forecasting as main driver for profitability (Cobon & Toombs, 2013). These patterns are not fully investigated for Namibia, as the South Atlantic convergence zone is less predictable than the intertropical convergence zone and that weather is affected by distance from oceans and altitudes (Barreiro et. al. 2002,2005;Taschetto & Wainer, 2008).

Methodology

Descriptive statistics of the rainfall dataset

Namibian receives rainfall in the summer months and generally receives more than 50% of the precipitation during January and February. The general rain comes from North East and declines towards the South West zones. Available annual precipitation data from central Namibia was used to illustrate historical rainfall pattern in Namibia.

Data from the Waterberg area were selected because of its completeness since 1895. Table 1 provides an overview of the data used, while Figure 1 shows the Waterberg rainfall variability of the annual rainfall in comparison to other rainfall stations, such as Windhoek and Kamanjab.

Table 1: Rainfall statistics of the Waterberg rainfall station (1895-2019)

Waterberg	Average	CV*	Below	Above
Rainfall	501.9mm	43.3%	< 393.2mm	>610.5mm
Occurrence	33.9%		38.7%	27.4%
Intensity	10.2mm/day	30.3%	7.8mm/day	11.7mm/day

* Note: the coefficient of variation (CV) used in this analysis shows the variability of rainfall, defined as the standard deviation divided by the mean.

The fluctuation between years is shown by the high percentage of CV. Specifically, it can be seen that only 33.9% of the years resulted in rainfall between 393.2mm to 610.5mm. Furthermore, Table 1 shows that the rainfall intensity in normal years are about 10.2mm/day of precipitation, while below average rainfall years can be described as low intensity of 7.8mm/day, which has a direct influence on the vegetation requirements.

Moving averages were used to obtain general observations. The information shows that Namibia had droughts periods around 1902, 1920, 1933, 1949, 1961, 1982, 1995 and presently probably the worst of all. Excessive rain occurred around 1910, 1923, 1934, 1954 and 2011. It is interesting to observe that the different rainfall stations presented similar patterns, although the western location suggests to enter the dry period earlier. It can be observed, that the trough of dry years existed for at least some years. Although with some deviations, it appeared that the period between 1900 and 2019 included 9 cycles of approximately 13 years or 4 severe cycles of 28 years. If that is true, we almost reached the end of the trough of the current cycle.

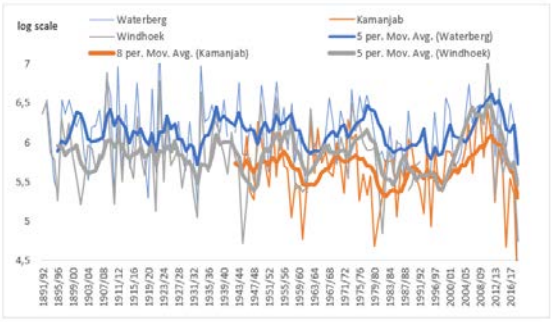

Figure 1: Moving averages of rainfall in Namibia[1].

Figure 2 presents the Waterberg annual rainfall in comparison to the ENSO effect (Kane, 2009), by applying a variable called the Southern Oscillation Index average (SOIA)[2]. This variable shows a significant but small correlation of 0.1752. To improve the correlation, we normalized the variable (see next section).

[1] The spectral characteristics of spatially averaged rainfall series

[2] The Southern Oscillation Index (SOI), gives an indication of the development and intensity of El Niño or La Niña events in the Pacific Ocean. The SOI is calculated using the pressure differences between Tahiti and Darwin. Sustained negative values of the SOI lower than −7 often indicate El Niño episodes. Sustained positive values of the SOI greater than +7 are typical of a La Niña episode. These monthly measures were aggregated as average annual measure to correspond to the Namibian rainfall season.

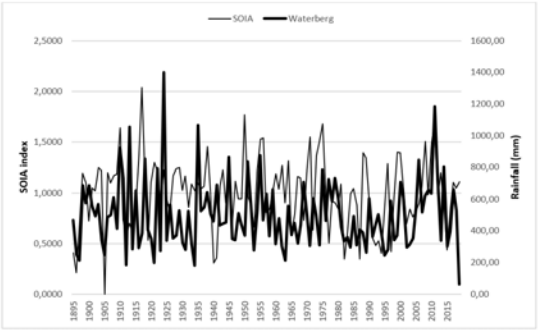

Figure 2: SOIA across the year relative to actual rain for Waterberg[3].

Time series modeling

Major improvements in the predictability of southern Africa's seasonal rainfall too place, specifically though the purely empirical-statistical approach and the dynamical approach to forecast rainfall. The statistical approach uses less computing resources and are based on relationships between the predicted and predictor variables (Shukla & Mooley, 1987, Krishnamurti et. al., 2002, Klotzbach & Gray, 2003, Sahai et. al., 2003, Annamalai et. al., 2005, Duffy et. al., 2006, Kim & Kim, 2010, Ye et. al., 2015, and Gerlitz et. al., 2016), while the dynamical approach is based on predicted rainfall as consistent with other climate variables (Doblas-Reyes et. al., 2006, Saha et. al., 2006). These approaches resulted into atmosphere–ocean coupled global circulation models and regional climate models being used as tools for dynamical (seasonal) rainfall prediction. Generally, studies have moved towards dynamical seasonal prediction (Misra, 2004, Pattanaik & Kumar, 2010, Yuan et. al., 2011; Liu et. al., 2013, Becker et. al., 2014, Siegmund et. al., 2015, Jia et. al., 2015, and Osman & Vera, 2017).

This paper used a combination of approaches to quantify the volatility in the rainfall series, effective rainfall, its intensity, cycles and the ENSO data. The methodologies developed in this study investigates the rainfall series from 1895 – 2018.

Normalising the outliners of variables

To account for the oscillation in patterns of the rainfall series over time, the study developed a model to fit the series (see Figure 3). The following equation is used.

$$R_j = \alpha_0 + \sum_{m=1}^{N} \left(\alpha_m \cos\frac{2\pi_j}{\theta_m} + \beta_m \sin\frac{2\pi_j}{\theta_m} \right) \quad (1)$$

$$0 \leq j \leq N, 1 \leq m \leq K$$

Where R_j is rainfall in any season j, α_m and β_m are parameters estimated in ordinary least regression, α_0 is the constant, N represent the total series size (years in the series)., K captures the number of prominent peaks in the spectrum of the rainfall series (see figure 2), and θ_m the period of periods of oscillation at each of the $m = 1 \ldots K$ peaks in the spectrum of the series.

The variable actual rain presents the normalization of the Waterberg rainfall. Its behavior illustrates a cyclical pattern data series is plotted in Figure 3, which shows that the actual rainfall mean seems to oscillate about $\theta_m = 34 \; and \; 48$ years, respectively. Equally, the accumulated rainfall cycle seems to oscillate about $\theta_m = 31 \; and \; 35$ years, respectively. These types of oscillation indicate volatility in rainfall; i.e. in the periods of crisis volatility is much higher. This clustering of volatility is a typical feature of rainfall in the face of uncertainty, which require precise modeling and forecasting.

[3] with spectral characteristics of spatially averaged rainfall series

The data have a particular feature in that the behaviour of the series changes over time. For example, Sartorius von Bach and Kalundu (2019) pointed out that a long-term cycle of 23 years follows a shorter cycle of 13 years, which has led to drastic shifts in biomass and gross margin value. Although such dramatic breaks are rare, one has to be aware of such shocks. For Namibia, a semi-arid country, rainfall cycles affect changes in biomass per hectare, leads to changes in stocking rate and farming decisions over time. It is upon these cycles that lead to changes into farming and agribusiness decision making process. The cycles as per Figure 3 and 4 illustrates these periods of serious policy decisions for the semi-arid country.

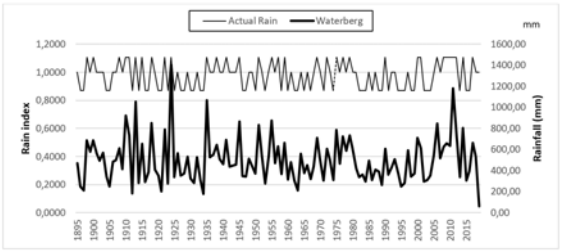

Figure 3: The A normalized actual rain cycle and the Waterberg rainfall

Based Dyer and Tyson (1977) and others, findings of cyclical rainfall patterns in Southern Africa (Du Toit & O'Connor, 2014 and Kane, 2009), a time series of accumulation of various cycles were used to analyse the Waterberg rainfall. This series called ACC, consists of 49-year, 21-year, 7-year and a 4-year cycles, and was normalized and presented in Figure 4.

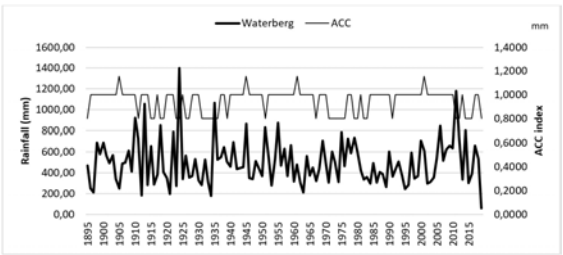

Figure 4: Cumulative rainfall cycles verse Waterberg rainfall

Ordinary least Square estimation

The next step was to develop econometric models to answer the postulation emphasized in this study. Firstly, the problem was based on the association of average rainfall and ENSO. It was argued here that the ordinary least squares (OLS) approach is sufficient to answer to the dependency of local rainfall patterns to the ENSO patterns (see Figure 3). This paper went further to explore the analysis in more robust dynamic modelling framework. OLS approach is precursor for underpinning a relationship that exists between regional rainfall periodicities, ENSO and cyclical pattern. Applying the concept of association, the OLS model was estimated to validate the claim that regional rainfall patterns is a function of ENSO and cyclical patterns. The assumptions are made in relation to the regression model is that they follow the Gauss-Markov assumption. The nature of the general equation is formulated as:

$$Y_i = \beta_1 + \beta_i X_t + \varepsilon_i \qquad (2)$$

The logarithm of the Waterberg rainfall as dependent variable (LW) in Y was assumed to be explained by three exogenous variables (X_i) denoting its normalized rainfall cycles (ACC), Actual rain and the variable SOIA. β_0 and β_i, are parameters to be estimated, while ε_i is the disturbance term. The coefficient of each X variable provides an estimate of its influence on Y, controlling for the effects of all the other X variables (Dougherty 2012).

Results and discussion

Ordinary least Square model results

Various approaches suggested in literature were selected before a robust model was found. The model summarized in Table 2 show F-statistics which is significant at 5 percent and adjusted R-Squared indicated that about 83 percent of variation in rainfall patterns in Waterberg is explained by the variation in the ENSO, ACC and actual rain. The model is rid of any form of serial correlation because the Durbin-Watson is greater than 2. Further, results from the OLS estimation indicates that rainfall patterns in Waterberg is dependent on oscillations of ENSO pattern, and the cycles of domestic climatic patterns. The occurrence of the El Niño Southern Oscillation accounts for 21 percent of the effect on the local rainfall.

Table 2: OLS result summary based on equation 2

Variable	Coefficient	Std. Error	t-Statistic	Probability
Constant	2.9092	0.1866	15.5714	0.0000*
ACC	-0.1941	0.1159	-1.6739	0.0967**
Actual Rain	3.4068	0.1435	23.7339	0.0000*
SOIA	0.2096	0.0909	2.3079	0.0227*
Adjusted R-Squared	0.8269			
F-statistics	196.8869			0.0000*
Durbin-Watson Stat	2.2844			

Note: * and ** denote that the variable is significant at 5 percent and 10 percent level, respectively.

Model performance

As stated in the method section, the model performance of individual behavioural equations were tested using both graphical and statistical techniques. The ability of a simulation model to correctly predict the key turning points in the actual data is an important criterion for model assessment (Lütkepohl & Krätzig (eds).2004).

The graphical result for model adequacy test is illustrated in Figure 6. The visual inspection of the estimated single equations have demonstrated that all the remaining estimated models perform well in capturing the turning points in the actual values. Statistical methods were also used to evaluate the robustness of our estimated models. Statistical approaches that examine forecasting ability of models largely assess forecast error value, which is obtained as the deviations of the forecast value from the actual value. A model that produce a low error value is considered as a sign of good forecasting ability and the results are qualified for using for forecasting and policy purposes (Lütkepohl, & Krätzig (eds).2004). The forecast evaluation was carried out using in sample period by using the historical periods from 2001 to 2015. We employed different forecast statistics to evaluate how well our model captures the real actual values. Following Lütkepohl & Krätzig (eds).2004, the following seven statistical techniques namely Mean Average Error (MAE), Mean Average Percentage Error (MAPE), Root Mean Squared Error (RMSE), Theil Inequality Coefficient (U), Bias, Variance and Covariance proportions were employed to evaluate the forecasting ability of the individual equations. The specifications for the first four methods are described below.

The Mean Average Error is computed as the average value of the absolute value of the error terms occurring in each period, and is given in equation 3:

$$MAE = \frac{1}{T}\sum_{t=1}^{T}|\hat{y}_t - y_t| \qquad (3)$$

On the other hand, the Mean Average Percentage Error (MAPE) captures the error in terms of percentage of the actual value. MAPE is calculated using equation 4:

$$MAPE = \frac{1}{T}\sum_{t=1}^{T}\left|\frac{\hat{y}_t - y_t}{y_t}\right| \quad (4)$$

The Root Mean Squared Error (RMSE) is the standard deviations of the forecast errors. RMSE is computed using the following formula:

$$RMSE = \sqrt{\frac{1}{T}\sum_{t=1}^{T}(\hat{y}_t - y_t)^2} \quad (5)$$

The other statistical method to evaluate the forecasting ability is the Theil Inequality Coefficient (U) (Theil, 1967). The formula used to compute U is specified in equation 6. The numerator of the formula is the root mean squared errors. The Theil Inequality Coefficient lies between 0 and 1, with 0 indicating a perfect fit. It is important to note that RMSE and MAE depend on scale of a dependent variable, while the next two statistics (MAPE and Theil Inequality Coefficient) are scale invariant.

$$U = \frac{\sqrt{\frac{1}{T}\sum_{t=1}^{T}(\hat{y}_t - y_t)^2}}{\sqrt{\frac{1}{T}\sum_{t=1}^{T}(\hat{y}_t)^2}\sqrt{\frac{1}{T}\sum_{t=1}^{T}(y_t)^2}} \quad (6)$$

Bias proportion indicates how far is the mean of the forecast from the mean of the actual series. Likewise, variance proportion indicates how far is the variance of the forecast from the variance of the actual series. Covariance proportion measures the remaining unsystematic forecasting errors. It is important to note that the bias, variance and covariance proportions add up to one and are given as proportions out of 1.

If the forecasts are said to be good, the bias and variance proportions should be small, which is the case in the estimated behavioural equation. The results for the forecast evaluation are given in Table 3.

Table 3: Forecast evaluation for the estimated model

Forecast statistics	Behavioural equation
	Rainfall
Theil Inequality Coefficient (U)	0.1524
Bias Proportion	0.0000
Variance Proportion	0.0596
Covariance Proportion	0.9404
Mean Absolute Percentage Error (MAPE)	2.0909
Mean Absolute Error (MAE)	0.1268
Root Mean Squared Error (RMSE)	0.1660

Source: Model output

The findings were fitted into Figure 5 to illustrate the actual and the forecast for the next 5 years (2019 to 2024). The reported forecast statistics value indicates that most of the forecast accuracy statistics using Theil's Inequality Coefficient (U) produced results closer to zero, which is an indication for good model forecast. In addition, the mean absolute percentage error is around and below ten percent for the remaining models. Hence it can be concluded that the single behavioural model performs reasonably well in tracking the actual values and therefore can be used for forecasting and policy analysis. Once we make sure that the model is adequate in approximating the rainfall patterns and ENSO, it is possible to proceed to analyse rainfall outlooks and simulation for the prospects of above normal, normal and below normal rainfall and its implications for agriculture in Namibia.

The forecast is depicted in figures 5 to 8. Figure 5 shows the historical series from 1895 to 2018, and a 5-year forecast, that from 2019 to 2024. The individual figures are explained in the subsequent sub-section.

with finding the strength and direction of the relationship (Beins & McCarthy, 2012).

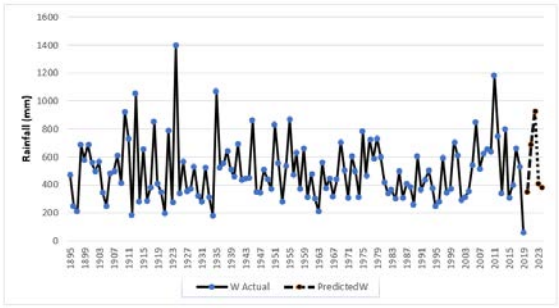

Figure 5: Depicts actual Waterberg rainfall and predicted rainfall

The modeling led to forecasting for the Waterberg area, which could be applied to changes into farming and agribusiness decision making process. The forecast show that for 2020, a slightly below average rainfall (refer to Table 1) can be expected, followed by 2 years of above average rainfall. To understand the cyclical pattern, Figures 6 to 8 extracted a 10-year period from Figure 5 to indicate how the selected normalized variables contribute to the forecast. The figures demonstrate the explanatory value towards the forecast of rainfall for Waterberg.

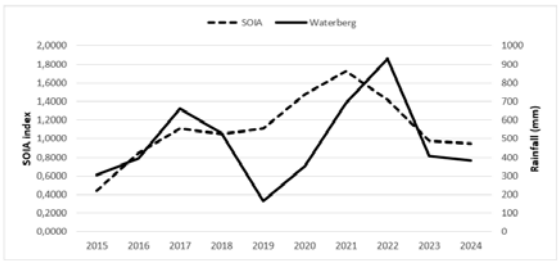

Figure 6: Depicts SOIA and Waterberg rainfall

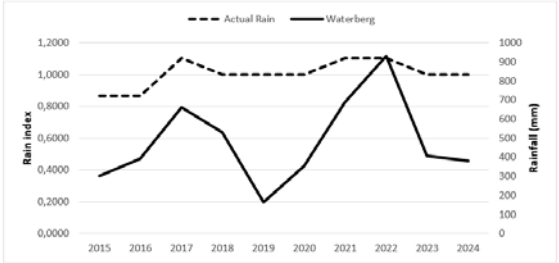

Figure 7: Depicts actual rain and Waterberg rainfall

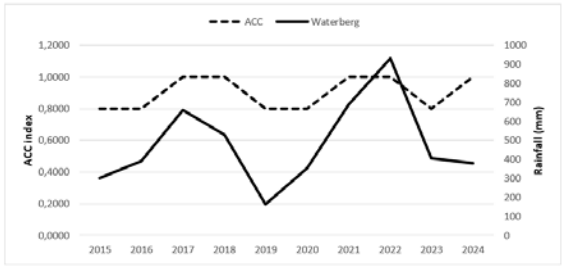

Figure 8: Depicts ACC and Waterberg rainfall

Conclusion

Using the existing literature suggestions, the paper contribute towards the rainfall prediction in Namibia. From the data it is clear that only 34% of the years resulted into average rainfall, thus 66% of rainfall is either above or below. These patterns call for more informed knowledge to be incorporated into targeted agricultural output and resultant decision making. The analysis shows that the ENSO patterns significantly affects the rainfall patterns in Namibia. Specifically, it shows that the ENSO follows a cyclical pattern, which corresponds to the Waterberg rainfall. Other normalised variables indicate that rainfall pattern follows cycles. It is shown here that forecasting is possible, by using existing data to contribute towards improved decision making. The 5-year forecast indicates that the Waterberg area expects drought in the first 2 years, then above average rainfall for at least 3 years. The findings of this paper confirm the findings of Ganguli and Coulibaly (2017) who indicates that further long-term cyclical effects of rainfall, weather and global warming information will be required for repeated model-runs to point out additional effects.

It is evident that further research is required for an early warning system of Namibia and the region. Knowledge of cyclical rainfall trends need to be translated into reliable statements about the likelihood of drought occurrences and the duration and its severity.

Such statements are of significant importance for the agricultural sector and national economic planning. Results emanating from rainfall periodicities can be used to safeguard against future famines, possible food shortages and to counter rising food prices.

Although the methods used are robust, they call for further research into the dynamic causes of observed rainfall variability. Access to reliable data is called for. This paper helps in stimulating the debate about applicable ways of understanding the bigger climate mechanisms behind hydrologic extremes, where countries without large computational and financial support can tap into available forecasts (see Mason & Tippett, 2017).

References

Anderson, T.M., Ritchie, M.E. & McNaughton S.J. (2007). Rainfall and soils modify plant community response to grazing in Serengeti National Park. *Ecology* 88 (5) 1191–1201.

Annamalai, H.J., Potemra, R. Murtugudde, & McCreary, J.P. (2005). Effect of preconditioning on the extreme climate events in the tropical Indian Ocean. J. *Climate*, 18, 3450–3469.

Arora, V.K., (2002). The use of the aridity index to assess climate change effect on annual runoff. J. *Hydrol.*, 265, 164–177.

Barreiro, M., Chang, P. & Saravanan, R. (2002). Variability of the South Atlantic convergence zone simulated by an atmospheric general circulation model. *J Climate* 15. 745-763.

Barreiro, M., Chang, P. & Saravanan, R. (2005). Simulated precipitation response to SST forcing and potential predictability in the region of the South Atlantic convergence zone. Climate Dyn., 24, 105–114.

Becker, E., van den Dool, H. & Zhang, Q. (2014). Predictability and forecast skill in NMME. J. Climate, 27, 5891–5906.

Bollerslev T. (1986). Generalized autoregressive conditional heteroskedasticity. *Journal of Econometrics*, 31(3), 307–327.

Box, G.E.P. & Jenkins G.M. (1976). Time Series Analysis: Forecasting and Control; Holden Day: San Francisco, CA, USA.

Chin W.Q. (1978). Drought cycles and weather patterns, *Canadian Water Resources Journal,* 3 (1) 68-84.

Cobon, D.H. & Toombs, N.R. (2013). Forecasting rainfall based on the Southern Oscillation Index phases at longer lead-times in Australia. *The Rangeland Journal,* 35, 373–383.

Cohen, J., Screen, J.A., Furtado, J.C., Barlow, M., Whittleston, D., Coumou, D., Francis, J., Dethloff, K., Entekhabi, D., & Overland, J. (2014). Recent Arctic amplification and extreme mid-latitude weather. *Nat. Geosci.* 7, 627–637.

Cottrill, A., Hendon, H.H., Lim, E.-P., Langford, S., & Shelton, K. (2013). Seasonal forecasting in the Pacific using the coupled model POAMA-2. *Weather. Forecasting*, 28, 668–680.

Crevits, R. & Croux, C. (2007). Forecasting Using Robust Exponential Smoothing with Damped Trend and Seasonal Components; Working Papers Department of Decision Sciences and Information Management 588812; Faculty of Economics and Business, Department of Decision Sciences and Information Management: Leuven, Belgium.

Diodato, N. & Bellocchi, G. (2018). Using Historical Precipitation Patterns to Forecast Daily Extremes of Rainfall for the Coming Decades in Naples (Italy). *Geosciences* 8(8), 93.

Doblas-Reyes, F.J., Hagedorn, R. & Palmer, T.N. (2006). Developments in dynamical seasonal forecasting relevant to agricultural management. *Climate* Res., 33, 19–26.

Duffy, P.B., Arritt, R.W. & Coquard, J. (2006). Simulations of present and future climates in the western United States with four nested regional climate models. J. *Climate*, 19, 873–895.

Du Toit, J. & O'Connor T.G. (2014). Changes in rainfall pattern in the eastern Karoo, South Africa, over the past 123 years. *Water* SA 40 (3) 543-460.

Dyer, T.G.J. & Tyson, P.D. (1977). Estimating above and below normal rainfall periods over South Africa, 1972-2000. *Journal of Applied Meteorology*, 16, 145-147.

Emiliani, C. (1966). "Paleotemperature Analysis of Caribbean Cores P6304-B and P6304-9 and a Generalized Curve for the Past 425, years." The *Journal of Geology,* 74 (2).

Engle R.F. (1982). Autoregressive conditional heteroskedasticity with estimation of the variance of UK inflation. *Econometrica*, 50(4), 987–1008.

Ganguli, P. & Coulibaly P. (2017). Does nonstationarity in rainfall require nonstationary intensity–duration–frequency curves? *Hydrol. Earth Syst. Sci.,* 21, 6461–6483.

Gao, X. & Giorgi F. (2008). Increased aridity in the Mediterranean region under greenhouse gas forcing estimated from high resolution simulations with a regional climate model. *Global Planet. Change*, 62, 195–209.

Gardner, E.S. Jr. (2006). Exponential smoothing: The state of the art—Part II. *Int. J. Forecast*. 22, 637–666.

Gerlitz, L., Vorogushyn, S., Apel, H., Gafurov, A., Unger-Shayesteh, K. & Merz, B. (2016). A statistically based seasonal precipitation forecast model with automatic predictor selection and its application to central and south Asia. *Hydrol. Earth Syst. Sci*., 20, 4605–4623.

Hirata, F.E. & Grimm, A.M. (2018). Extended-range prediction of South Atlantic convergence zone rainfall with calibrated CFSv2 reforecast. *Climate Dyn.*, 50, 3699–3710.

Hollinger, S.E.., Isard, S.A. & Welford, M.R. (1993). A new soil moisture dryness index for predicting crop yields. Eighth Conf. on Applied Climatology, Anaheim, CA, *Amer. Meteor. Soc*., 187–190.

Holt, C.C. (2004). Forecasting seasonal and trends by exponentially weighted moving averages. *Int. J. Forecast*. 20, 5–10.

Hyndman, R.J., Koehler, A.B., Ord, J.K., & Snyder, R.D. (2008). Forecasting with Exponential Smoothing: The State Space Approach; Springer: Berlin, Germany.

Jia, L., Yang, X., Vecchi, G.A., Gudgel, R.G., Delworth, T.L., Rosati, A., Stern, W.F., Wittenberg, A.T., Krishnamurthy, L., Zhang, S., Msadek, R., Kapnick, S., Underwood, S., Zeng, F., Anderson, W.G., Balaji, V., & Dixon, K. (2015). Improved seasonal prediction of temperature and precipitation over land in a high-resolution GFDL climate model. *J. Climate*, 28, 2044–2062.

Kane, R.P. (2009). Periodicities, ENSO effects and trends of some South African rainfall series: an update. *South African Journal of Science*. 105, 199-207

Kim, H.-M., &. Kim, Y.-H. (2010). Seasonal prediction of monthly precipitation in China using large-scale climate indices. *Adv. Atmos*. Sci., 27, 47–59.

Klotzbach, P.J., & Gray, W.M. (2003). Forecasting September Atlantic basin tropical cyclone activity. *Wea. Forecasting*, 18, 1190–1128.

Krishnamurti, T.N., Stefanova, L. & Chakraborty, A. (2002). Seasonal forecasts of precipitation anomalies for North American and Asian monsoons. *J. Meteor*. Soc. Japan, 80, 1415–1426.

Lin, L.; Wang, Z.; Xu, Y.; Fu, Q. (2016). Sensitivity of precipitation extremes to radiative forcing of greenhouse gases and aerosols. *Geophys*. Res. Lett. 43, 9860–9868.

Liu, X., Yang, S., Li, Q., Kumar, A., Weaver, S. & Liu, S. (2013). Sub-seasonal forecast skills and biases of global summer monsoons in the NCEP Climate Forecast System version 2. *Climate Dyn*., 42, 1487–1508,

Lütkepohl, H. & Krätzig, M. (eds). (2004). Applied time series econometrics. Cambridge University Press.

Mason, S.J., & Tippett, M.K. (2017). Climate predictability tool version 15.5.10. International Research Institute for Climate and Society, Columbia University.

McClain, J.O. (1974). Dynamics of exponential smoothing with trend and seasonal terms. *Manag*. Sci. 20, 1300–1304.

McKee, T.B., Doesken, N.J. & Kleist, J. (1993). The relationship of drought frequency and duration to time scales. Eighth Conf. on Applied Climatology, Anaheim, CA, Amer. Meteor. Soc., 17–22.

Mishra, A.K. & Singh, V.P. (2010). A review of drought concepts. J. *Hydrol*., 391, 202–216.

Misra, V. (2004). An evaluation of the predictability of austral summer season precipitation over South America. *J. Climate*, 17, 1161–1175.

Monfared, M.A.S., Ghandali, R. & Esmaeili, M. (2014). A new adaptive exponential smoothing method for non-stationary time series with level shifts. *J. Ind.* Eng. 10, 209-216.

Nastos, P.T., Politi, N. & Kapsomenakis, J. (2013). Spatial and temporal variability of the aridity index in Greece. *Atmos*. Res., 119, 140–152.

Neusser, K. (2016). Time series econometrics, Springer. New York

Novella N.S. & Thiaw W.M. (2016). A seasonal rainfall performance probability tool for famine early warning systems. *Journal of applied meteorology and climatology*. 55 (12).

Palmer, W.C. (1965). Meteorological drought. Weather Bureau Research Paper 45, 58 pp. https://www.ncdc.noaa.gov/temp-and-precip/drought/docs/palmer.pdf.

Palmer, W.C. (1968). Keeping track of crop moisture conditions, nationwide: The new crop moisture index. *Weatherwise*, 21, 156–161.

Pattanaik, D.R. & Kumar, A. (2010). Prediction of summer monsoon rainfall over India using the NCEP climate forecast system. *Climate Dyn*., 34, 557–572.

Rowell, D.P., Senior, C.A., Vellinga, M. & Graham, R.J. (2016). Can climate projection uncertainty be constrained over Africa using metrics of contemporary performance? *Climatic Change*, 134, 621–633.

Saha, S., Moorthi, S., Wu, X., Wang,J., Nadiga,.S., Tripp, P., Behringer, D., Hou, Y.-T., Chuang, H., Iredell, M., Ek, M., Meng, J., Yang, R., Mendez, M.P., van den Dool, H., Zhang, Q., Wang, W., Chen, M. & Becker, E. (2014). The NCEP Climate Forecast System version 2. *J. Climate*, 27, 2185–2208.

Sahai, A.K., Grimm, A.M., Satyan, V. & Pant, G.B. (2003). Long-lead prediction of Indian summer monsoon rainfall from global SST evolution. *Climate Dyn*., 20, 855–863,

Sartorius von Bach, H.J. & Kalundu, K.M. (2019). An econometric estimation of gross margin volatility: A case of ox production in Namibia, Contributed paper to 57th AEASA conference, Bloemfontein, RSA, and submitted to Agrekon.

Shukla, J., & Mooley, D.A. (1987). Empirical prediction of the summer monsoon rainfall over India. *Mon. Wea. Rev.*, 115, 695–703.

Yusof, F. & Kane, I.L. (2012). Volatility modeling of rainfall time series. Theoretical Applied Climatology, DOI:10.1007/s00704-012-0778-8

Siegmund, J., Bliefernicht, J., Laux, P. & Kunstmann, H. (2015). Towards a seasonal precipitation prediction system for West Africa: Performance of CFSv2 and high-resolution dynamical downscaling. J. *Geophys. Res. Atmos*., 120, 7316–7339.

Taschetto,A.S., & Wainer, I. (2008). Reproducibility of South American precipitation due to subtropical South Atlantic SSTs. *J. Climate*, 21, 2835–2851.

Taylor, J.W. (2003). Exponential smoothing with a damped multiplicative trend. *Int. J. Forecast*. 19, 715–725.

Theil, H. (1967). Economics and Information Theory, Amsterdam, North Holland.

Um M.-J., Kim, Y., Park, D. & Kim J. (2017. Effects of different reference periods on drought index (SPEI) estimations from 1901 to 2014 *Hydrol. Earth Syst. Sci*., 21, 4989–5007.

Walker, G.T. (1923). World Weather I. *Mem. Indian Meteor*. Dep., 24, 75–131.

Winsemius, H.C. Dutra E., Engelbrecht, F.A., Van Garderen E.A., Wetterhall F., Pappenberger F. & Werner M.G.F. (2014). The potential value of seasonal forecasts in a changing climate in southern Africa. *Hydrol. Earth Syst. Sci.,* 18, 1525–1538.

Ye, K.-H., Tam, C.Y., Zhou, W. & Sohn, S.J. (2015). Seasonal prediction of June rainfall over South China: Model assessment and statistical downscaling. *Adv. Atmos. Sci*., 32, 680–689.

Yuan, X., Wood, E.F., Luo, L. & Pan, M. (2011). A first look at Climate Forecast System version 2 (CFSv2) for hydrological seasonal prediction. *Geophys*. Res. Lett., 38, L13402.